Tidal Turbine Blade Load Experiments for Oscillatory Motion

Ian A. Milne[a*], Alexander H. Day[b], Rajnish N. Sharma[a], Richard G.J. Flay[a] and Simon Bickerton[a]
[a]Department of Mechanical Engineering
The University of Auckland, Auckland 1010, New Zealand
*E-mail: imil015@aucklanduni.ac.nz
[b]Department of Naval Architecture and Marine Engineering
University of Strathclyde, Glasgow G4 0LZ, United Kingdom
E-mail: sandy.day@strath.ac.uk

***Abstract*—This paper presents blade root bending moment measurements of a horizontal-axis tidal turbine for planar oscillatory motion, conducted in a stationary water towing tank.**

By comparing the measurements with quasi-steady reconstructions for both single and multiple frequency oscillatory motion, the bending moment was shown to be sensitive to both frequency and amplitude, as well as to the mean tip-speed ratio. The unsteady loads associated with the separation of the flow and dynamic stall are shown to be of considerably greater importance than those which are already present for attached flow, such as added mass and dynamic inflow. A linear model fit to the unsteady bending moment also indicates that the inertia contribution is relatively small.

For cases where attached flow exists over the majority of the load cycle, these reconstruction methods are likely to be sufficient to obtain a reasonable prediction of the root out-of-plane bending moment. However, turbines whose blades are likely to operate near stall are likely to require more complex models for accurate load predictions to mitigate the risk of fatigue failure.

***Index Terms*—Tidal turbine, unsteady hydrodynamic loads, added mass, dynamic inflow, dynamic stall**

I. Introduction

A. Background and objectives of the present study

This paper presents results of an experimental based study which investigated the sensitivity of the blade loads of a scale model tidal turbine to unsteady planar motion.

Unsteadiness in the onset flow is a dominant driver of the fatigue loads of tidal turbine blades, arising from turbulence, surface waves and a depth-wise variation in the mean flow [1]–[4]. Characterising the unsteady blade loads is of utmost interest for tidal turbine designers, who are currently seeking to reduce high levels of conservativeness and improve the economic viability of the industry.

Indicative of a developing technology, there is yet no clear consensus as to the preferred operational strategy for a tidal turbine. Some turbine developers have preferred simple devices with few moving parts in an attempt to reduce offshore maintenance costs, typically being stall regulated and employing fixed pitch blades. Recognising that the blade loads at high flow speeds are a dominant source of fatigue, other designers have chosen to pursue more complex devices, with blade pitch actuation. A greater understanding of the unsteady loads will therefore aid developers in selecting their preferred operational strategy.

In contrast to the loads experienced in steady flow conditions, additional forces are induced for a time variant onset flow. At the blade section level, true added mass effects are present due to the change in the pressure field of the fluid around the blade. At high angles of attack near stall the performance can also differ significantly from that for a static foil, with the delay and reattachment of the flow, leading to notable hysteresis loops. In terms of the wake, inertia effects result in a time lag between a new equilibrium in the wake induction being reached following a change in loading, a phenomenon commonly referred to as dynamic inflow.

The objective of this present study was to experimentally analyse the bending moment response to single and multiple frequency oscillations, for a various perturbation amplitudes and operational states. By comparing the unsteady bending moment with quasi-steady and linear based reconstructions, there was also the aim to attempt to quantify the relative influence of the various unsteady load constituents. This will therefore assist blade designers in evaluating the level of complexity required in their load prediction models.

B. Literature review

Whilst the steady thrust loads of tidal turbine blades are reasonably well understood [5]–[8], literature pertaining to unsteady rotor loading in general, and more specifically the unsteady blade loads is relatively scarce. Acknowledging that the added mass and dynamic inflow affects are likely to have more significance for a tidal turbine than a wind turbine due to the differences in fluid density, Whelan [9] recently has experimentally investigated the unsteady thrust forces of a tidal turbine subject to planar oscillatory motion in a flume. It was shown that the combined thrust forces due to true added mass and dynamic inflow, were negligible compared to the force in phase with velocity. Using a simplified theoretical model based on unsteady airfoil theory, it was also hypothesised that for a full-scale turbine, the force contribution from dynamic inflow acts in opposition to that of true added mass.

Investigations of the unsteady response of tidal turbines have also been performed in stationary water towing tank facilities.

For such tests there is no depth-wise shear profile, and relatively little turbulence. The incident flow is therefore more uniform over the rotor and more suited to planar oscillatory tests. Galloway et al. [10] have reported on experiments on a scale model turbine exposed to surface waves, where for relatively small waves of approximately 1.6m fullscale, the cyclic shaft thrust range was relatively large and in the order of 37 percent of the mean.

Inferring the hydrodynamic loading from shaft measurements however, has the implication that the contributions of the shaft and hub inertia are also present and must be accounted for. Barltop et al. [11] have instead directly obtained the blade root bending moment response using instrumented blades. They have also reported on a set of experiments in stationary water, where the turbine the was subject to velocity perturbations from surface waves. The bending moment time histories were found to compare reasonably well with a numerical blade-element momentum model based on a equilibrium wake model, again suggesting than unsteady influences were small.

Literature on the dynamic stall phenomenon of rotating blades is currently restricted to the wind turbine and helicopter contexts. Shipley et al. [12] inferred the dynamic stall occurrence of a wind turbine blade under various inflow conditions from pressure measurements on the blade surface. Leishman [13], [14] has also provided an in depth discussion of flow morphology associated with dynamic stall and references a number of experimental studies of oscillating 2-D airfoils in wind tunnels. There is an apparent need to establish the operating conditions in which dynamic stall is likely to be instigated for tidal turbines, and the load ranges which result.

II. Experimental set-up and data acquisition

A. Specifications of the towing tank and main carriage

The experiments for this present study were conducted at the Universities of Glasgow and Strathclyde's 76m long, 4.6m wide, 2.5m deep, still water towing tank. For all tests the water depth was maintained at 2.3m. A 9m long beach is installed at one end of the tank, with reflection coefficient typically less than 5%. The main carriage velocity is computer controlled, and was ramped up at constant acceleration at the start of each test, and then maintained constant for the duration of the test period, before being ramped down again.

B. Specifications of the sub-carriage

The main carriage is equipped with a digitally-controlled sub-carriage, which is shown in Fig. 1. The sub-carriage is driven by a linear actuator, and with a comparatively low inertia compared to the main carriage, can produce accelerations in the order of $2g$. For the present tests an oscillatory displacement time history was input into the computer controlling the sub-carriage, such that the desired upstream velocity of the turbine was of the form

$$u(t) = U + \sum_{i=1}^{n} \mu_i U \cos\left(2\pi f_i \cdot t + \phi_i\right), \qquad (1)$$

where U is the velocity of the main carriage, μ_i $(= u_{max}/U)$ is the current number of frequency component f_i and ϕ is a phase angle.

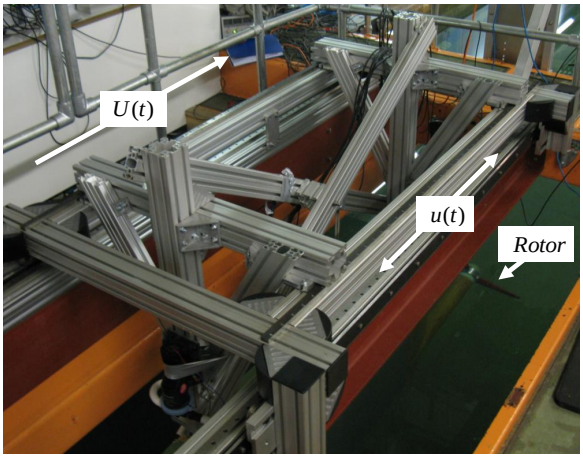

Fig. 1: Main towing carriage and sub-carriage, with turbine installed below.

C. Specifications of the turbine and blades

The horizontal-axis turbine is tri-bladed, with a rotor diameter of 780mm, and is shown in Fig. 2. The turbine motor, slip ring, and thrust and torque transducer are enclosed in a rectangular box at a distance of approximately 2 diameters downstream of the rotor. The box was mounted rigidly to the sub-carriage from above, and the rotor axis was 0.70m below the mean free water surface.

The rotor blades have a non-uniform profile, with the chord and twist varying along the span. The blade section geometry conforms to the NREL 814 airfoil [15], with a constant thickness of 20 percent of the local chord. Each of the three blades were instrumented with strain gauges installed on the cylindrical blade root, and enclosed within the rotor hub.

The rotational speed was controlled digitally, and was held constant for each test. The oscillatory motion of the sub-carriage therefore induces a perturbation in both the tip-speed ratio and the rotor torque.

D. Data acquisition and filtering

A Cambridge Electronic Design Power1401 data acquisition system, with a sampling rate of 400Hz was used to acquire all signals, except from the velocity of the main carriage. A low pass digital filter with a cut-off frequency of 300Hz was applied in real time on all signals. Once acquired, an IFR 5th order Butterworth digital filter was also applied off-line to all signals co-currently, and in both forward and backward directions to eliminate any phase error. The cut-off frequency was set at 5 times the highest oscillatory frequency, which was found to reduce erroneous noise, whilst ensuring that any stall events and non-sinusoidal motions were retained.

Fig. 2: Turbine used in experiments prior to being installed in tank, with main towing carriage in background. Motor, slip ring, and thrust and torque transducer are enclosed in the box at rear.

III. Rotor performance and blade loads for steady velocity

The rotor power and thrust, and blade loads were characterised for conditions indicative of steady flow, at a range of constant rotor speeds. With the sub-carriage disabled, the main carriage velocity was varied between U=0.45-1.01 m/s. These velocities are equivalent to full-scale velocities U=2.01-4.52 m/s assuming Froude number based scaling and a geometric scale ratio of 20:1. Issues with water spillage from the tank imposed an upper limit on the carriage velocity and hence the minimum tip-speed ratio able to be considered.

The non-dimensional power P(=ΩR), thrust (T), and in-plane (M_x) and out-of-plane (M_y) blade root bending moment curves, as a function of tip-speed ratio are presented in Fig. 3. The coefficients are defined as

$$C_P = \frac{P}{0.5\rho A U^3}, \tag{2}$$

$$C_T = \frac{T}{0.5\rho A U^2}, \tag{3}$$

and

$$C_M = \frac{M}{0.5\rho A R U^2}, \tag{4}$$

where A is the frontal area of the rotor and R is the rotor radius.

The curves are characterised by a relatively steep decay at low tip-speed ratio, where stall effects are dominant. The optimal power coefficient is attained at a tip-speed ratio between approximately $\lambda = 3-4$. At higher-tip speed ratios drag forces tend to dominate, leading to a reduction in the power coefficient, but an increase in the thrust and out-of-plane bending moment coefficients.

The coefficients also indicate sensitivity to the rotational speed, and therefore to the Reynolds numbers. For the highest rotor speed considered, of 96rpm, the Reynolds number at a blade section at $0.75R$, where the chord is approximately $c = 0.027m$, is estimated to range from $Re = 1.66 - 1.62 \times 10^5$. At the slowest rotor speed, the equivalent Reynolds number would have varied from $Re = 1.11 - 1.07 \times 10^5$. At this lower rotational speed, one would expect that the lift and drag performance of the foil would be reduced as the boundary layer nears a laminar flow regime. The increase in the thrust and out-of-plane bending moment coefficients at very high tip-speed ratios for the low rotor speed cases may be due to the influence of the brake state, where the thrust forces are more sensitive to global drag effects, rather than to the flow over the blade section.

The magnitude of the out-of-plane bending moment coefficient is considerably larger than the in-plane component, and is indicative of the dominance of the thrust forces over the gravitational and centrifugal inertia forces. Literature also suggests that it is the large load cycles, due to the hydrodynamic thrust forces, which are likely to contribute the greatest to fatigue of composite turbine blades [16]. It is for this reason that the remainder of this paper is directed towards characterising the out-of-plane root bending moment only.

IV. Blade load response to oscillatory motion

A. Sensitivity to oscillatory parameters

The influence of oscillatory motion on the blade root out-of-plane bending moment is first investigated for single frequency rotor oscillations. Given the finite length of the towing tank, each test comprised of at least 10 complete oscillations, excluding the load histories of the initial two oscillations after the steady velocity of the main carriage had been attained. Fig. 4 demonstrates the high repeatability in the individual oscillatory cycles which was able to be achieved. One can also observe that for the higher oscillatory frequencies considered the velocity and therefore acceleration time histories are not perfectly harmonic. This is due to physical constraints with the linear actuator on the sub-carriage, and introduces a higher frequency component to the time histories.

The sensitivity of the blade loads to the oscillatory frequency can be inferred from the bending moment history of an individual oscillation as a function of the instantaneous tip-speed ratio, which is in the form of a hysteresis loop. These loops are shown in Fig. 5 for a mean carriage velocity of $U = 0.78\ m/s$ and oscillatory frequencies ranging from $f = 0.45\ Hz$, to that corresponding to the rotational frequency of the rotor (1P). The frequencies are considered to be representative of those which would be induced by regular surface waves, and from the rotational sampling of turbulence [2], or from the depth-wise mean velocity profile. At 75% span, where the chord $c = 0.041m$, these oscillations

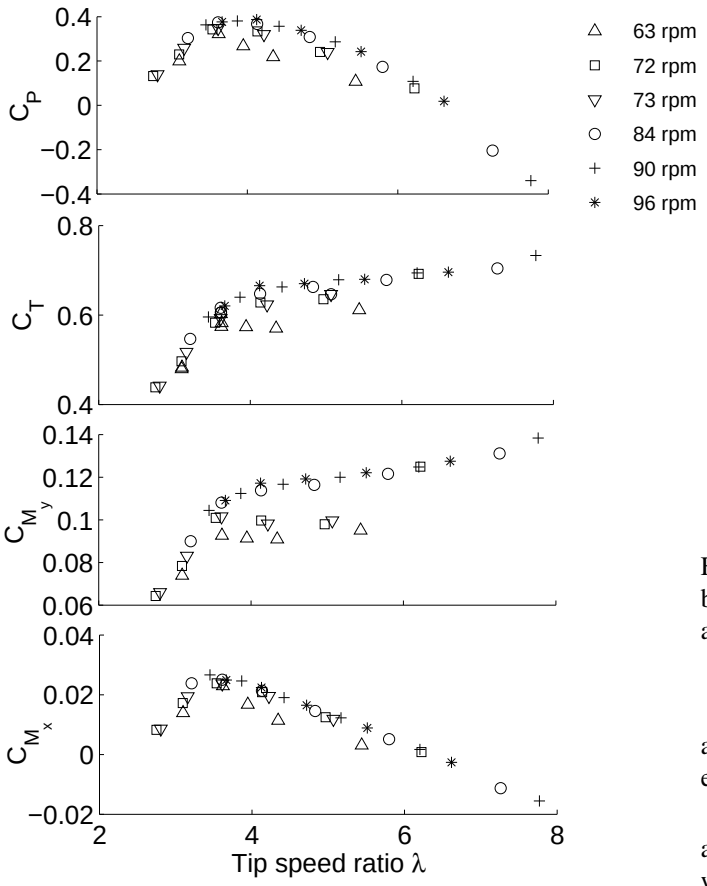

Fig. 3: From top: rotor power, thrust, and blade root out-of-plane and in-plane bending moment coefficients for steady carriage motion and constant rotor speeds. The gravitational load component has been removed from the in-plane bending moment.

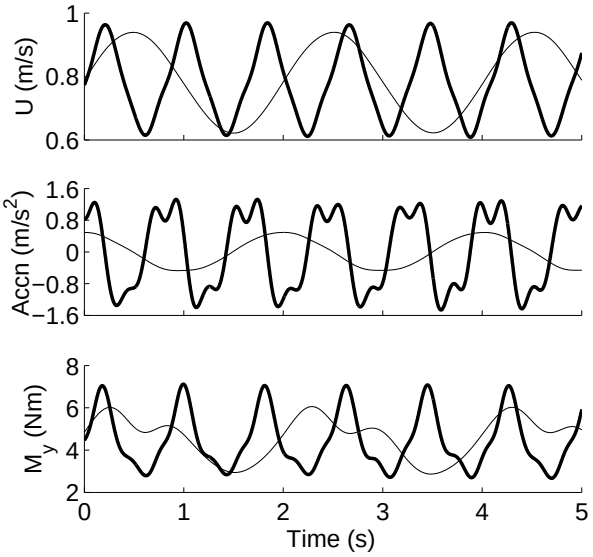

Fig. 4: From top: Velocity, acceleration and root out-of-plane bending moment time histories for $U = 0.78m/s$, $\mu = 0.2$ and two frequencies $f = 0.45\ Hz$, and $f = 1.1\ Hz$ (bold)

are representative of reduced frequencies $k(= \ cf\pi/V_{rel})$ ranging from $k = 0.031$ and $k = 0.026$, at a mean tip-speed ratio of $\lambda = 3.6$ and 4.1 respectively, to $k = 0.077$.

The corresponding quasi-steady bending moment is also plotted for each oscillatory cycle. To permit this, a smoothing spline was first fitted to the bending moment response for steady carriage motion. Linear interpolation was then used to obtain the bending moment corresponding to the instantaneous tip-speed ratio. For the unsteady load cases the instantaneous bending moment coefficient is defined herein as

$$C_{M_y} = \frac{M_y}{0.5\rho A U_{max}^2 R}. \tag{5}$$

One can observe the dominant hysteresis effects at low tip-speed ratio, where the flow has separated and the blade has stalled. In these conditions the magnitude of the unsteady bending moment is significantly greater than that which would be expected based on quasi-steady data. The point of flow separation and reattachment indicates a sensitivity to frequency, and for the highest frequency considered, the influence of stall effects appears to persist for much of the oscillatory cycle.

For cases where the flow does not completely separate, and for fully attached flow, the load history is relatively well described using quasi-steady predictions. This appears to suggests that for these conditions the influence of unsteadiness is relatively small.

Based on Theodorsen theory, for an foil subject to oscillatory motion, the load amplitude would be predicted to decrease with increased reduced frequency. One can observe that for the lower mean tip-speed ratio case, the load histories agree with this, in that the load troughs of the unsteady load are of greater magnitude than predicted by the quasi-steady model. For the higher mean tip-speed ratio case, the unsteady load magnitudes are however of smaller magnitude. This may be as a result of a quasi-steady brake state not being realised.

The effect of the oscillatory amplitude is analysed in Fig. 6, for two mean flow speeds and at an oscillatory frequency of $f = 0.89\ Hz$. These oscillatory amplitudes are considered to represent those which would likely be induced by regular surface waves, or large turbulent eddies. The point of flow separation and attachment is shown be a function of the current number, or in essence, whether the blade experiences shallow or deep stall. For a current number of $\mu = 0.1$, the non-harmonic oscillatory velocity is a dominant contributor to the irregularity observed in the dynamic load. One can also observe that at the highest velocity and rotational speed considered, stall occurs twice for the $\mu = 0.3$ case. This double stall phenomenon is not observed for $U = 0.67m/s$ case, and is likely due to the difference in the reduced frequency, which is $k = 0.06$, compared to $k = 0.04$ for $U = 0.89\ m/s$.

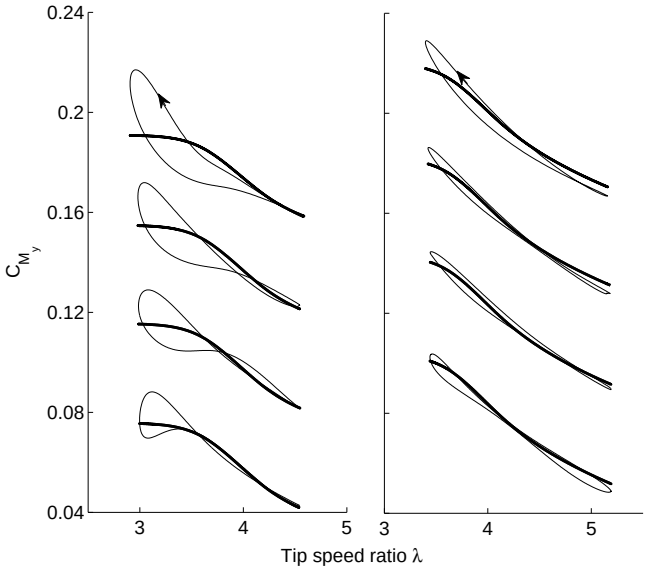

Fig. 5: Root out-of-plane bending moment coefficient as a function of instantaneous tip-speed ratio and a quasi-steady reconstruction (bold), for a mean velocity of $U = 0.78$ m/s and mean tip-speed ratio of λ=3.6 (left) and λ=4.1 (right). From bottom; f=0.50 Hz, f=0.64 Hz (offset by C_{M_y}=0.04), f=0.89 Hz (offset by C_{M_y}=0.08), and f=1P (offset by C_{M_y}=0.12).

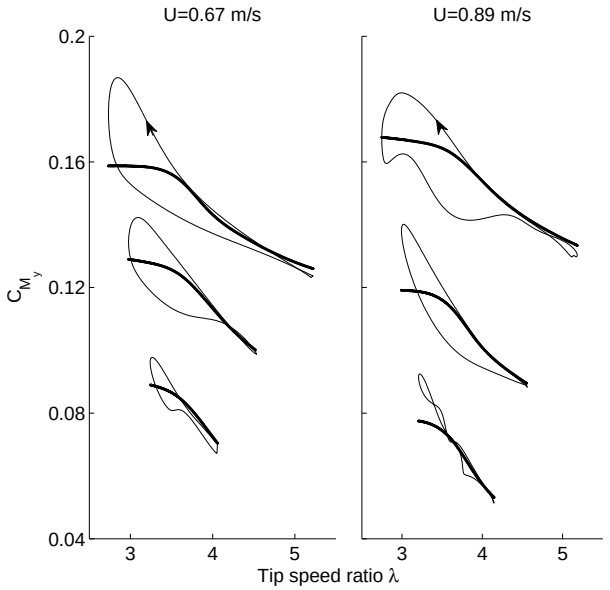

Fig. 6: Root out-of-plane bending moment coefficient as a function of instantaneous tip-speed ratio and a quasi-steady reconstruction (bold), for a mean tip-speed ratio of λ=3.6 and oscillatory frequency of $f = 0.89\ Hz$. From bottom; $\mu = 0.1$, $\mu = 0.2$ (offset by C_{M_y}=0.05) and $\mu = 0.3$ (offset by C_{M_y}=0.1).

B. Forces in phase with acceleration for attached flow

Whilst the forces in phase with acceleration in attached flow have been shown to be relatively insignificant, an attempt has been made to estimate their magnitude by fitting a linear model to the time history. This has initially been attempted for the single frequency oscillations at a mean tip-speed of λ=4.1 and current number of μ=0.1, where the flow is attached for the majority of the oscillation. An extension of the traditional form of Morison's equation [17] for an oscillating body in stationary water is employed here, in which the drag coefficient has been separated into both mean (C_v) and oscillatory components ($C_{v'}$), and there is no Froude-Krylov force component combined with the inertia force. The model, expressed in Eqn. 6, has been applied to the blade root bending moment by assuming equal loading over all three blades and the equivalent radius of $2/3R$. A least sum of squares fitting method, applied to the full oscillatory time history, has been used to compute the coefficients.

$$M_y = C_v \frac{1}{9}\rho A R U^2(t) + C_{v'} \frac{1}{9}\rho A R u'(t)\, U(t) + C_I \frac{2}{9}\rho V R \dot{u}(t)\,, \tag{6}$$

where V is the volume of a sphere with a radius equivalent to that of the rotor.

The oscillatory velocity and inertia coefficients are shown in Fig. 7, and an example time history of a reconstruction attempt can be observed in Fig. 8. The inertia coefficients,

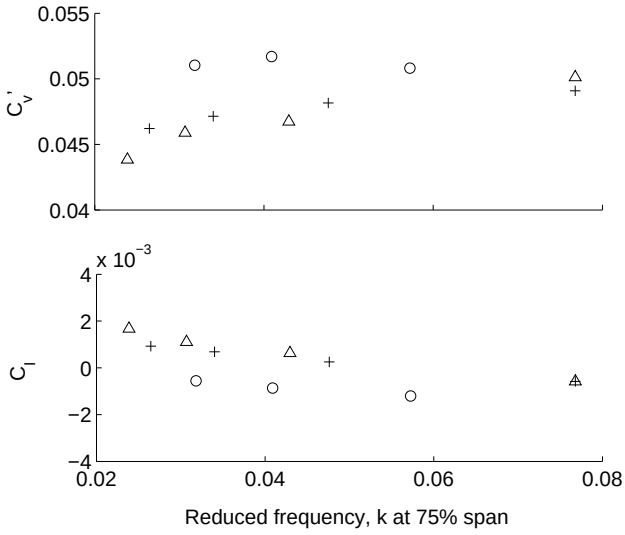

Fig. 7: Oscillatory and inertia coefficients for single frequency oscillations at μ=0.1 and a mean tip-speed ratio λ=4.1 U=0.67 m/s (o), U=0.78 m/s (+) and U=0.89 m/s (△).

and therefore the relative contribution to the unsteady load, are comparatively much smaller in magnitude than the drag coefficients, they also display a decreasing trend with reduced frequency. For the slowest rotor speed considered, and for the highest reduced frequencies of the two higher rotor speeds, the

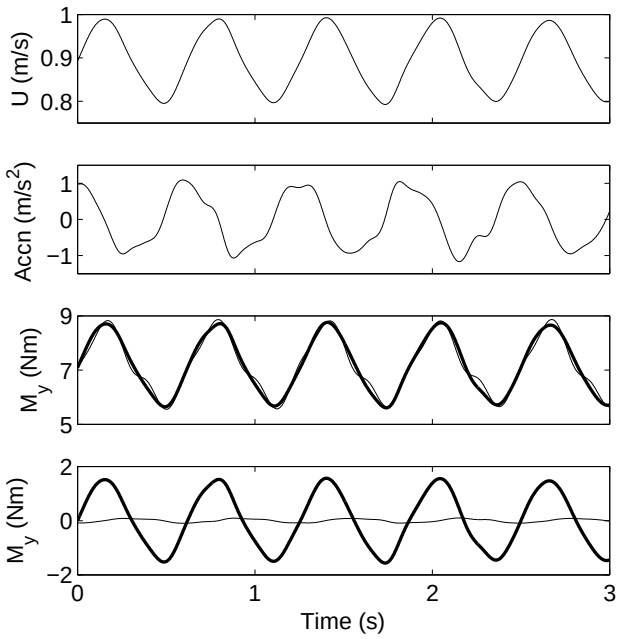

Fig. 8: Root out-of-plane bending moment reconstruction attempt for a single frequency oscillation case using a modified version of Morison's equation. U=0.89 m/s, λ=4.1, μ=0.1, k=0.077. From top; velocity; acceleration; measured and reconstructed bending moment (bold); and individual reconstructed bending moment components of oscillatory velocity (bold) and oscillatory inertia.

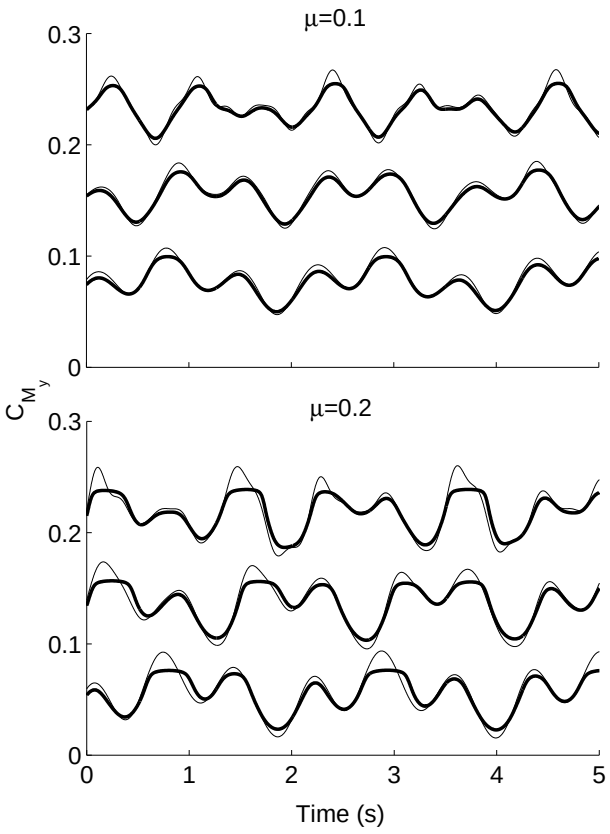

Fig. 9: Time histories of root out-of-plane bending moment coefficient of multi-frequency oscillations for U=0.78m/s and λ=4.1. From bottom; f=0.50 Hz, f=0.64 Hz (offset by $C_{M_y} = 0.1$) and f=0.89 Hz (offset by $C_{M_y} = 0.2$). All frequencies combined with f=1P. Dashed line represents a quasi-steady reconstruction

inertia forces are shown to act in opposition to the direction of acceleration. This decreasing trend agrees quantitatively with that which would be predicted using the unsteady airfoil theory presented by Whelan [9]. However, as previously discussed, for these cases of μ=0.1, the non-sinusoidal velocity will have an influence on these coefficients. To illustrate this, in Fig. 8 a slight irregularity can be observed in the velocity, acceleration and measured bending moment at the lower portion of the reverse cycle. The response is not completely modelled using the linear reconstruction, suggesting that there is a degree of non-linearity present in the blade and wake response. The effect of this hesitation on the load response appear to be similar to that expected from stall, which can make separating the two contributions challenging if they are both present.

C. Response to multiple frequency oscillations

The analyses are now extended to more complex cases, of oscillatory motion composed of two fundamental frequencies superimposed. For these analyses an integer number of complete oscillatory cycles were unable to be performed, however, the test duration was sufficient to again permit parametric investigations into the role of unsteadiness.

The sensitivity of the bending moment to both the oscillatory frequency combination and the amplitude segment of the blade root bending moment time history and corresponding quasi-steady is shown in Fig. 9, for a mean velocity of $U = 0.78\ m/s$ and tip-speed ratio of $\lambda = 4.1$. For these cases a $f = 1P$ frequency has been superimposed with the lower oscillatory frequencies previously considered, of $f = 0.50, 0.64, 0.89\ Hz$.

As for the single frequency cases, the quasi-steady model significantly under-predicts of the unsteady loading during stall, but offers much better predictions of the attached flow. Near the troughs the unsteady load tends to be consistently smaller compared to the the quasi-steady case, as was observed for the single frequency oscillations. However for the peaks in which the flow is still likely to be attached, the unsteady load appears to be greater than the quasi-steady case, in contrast to that which would be expected for single oscillations. Preliminary analyses suggest that this could be a result of dynamic inflow being more influential for multiple frequency oscillations.

V. Discussion

This study aimed to analyse the role of unsteady hydrodynamic forces on the blade loads of tidal turbines, which will aid tidal turbine designers in gaining confidence in load predictions and the applicability of simple models.

The unsteady loads associated with stall appear to dominate. Tidal turbines which are therefore stall regulated or are likely to operate in conditions where stall may be experienced, unsteady loads of considerably larger magnitude than that which would be predicted by a quasi-steady model can occur. The implications of this are that the blades of such turbines may be prone to enhanced rates of fatigue, and necessitate more complex load models for predicting seperated flow and dynamic stall. For turbines which operate with predominately attached flow across the blade one would expect a quasi-steady model to likely be sufficient, possibly with a correction factor to account for any differences. Whilst this would make load predictions relatively straightforward to attain, the turbine would likely have to be much more complex and incorporate active pitch control, and sited in flows not affected by large surface waves and strong turbulence.

The attempts which been made to establish the unsteady load contribution in attached flow due to acceleration effects, tend to agree quantitatively with unsteady airfoil theory. For the relatively high oscillatory frequencies tested, the non-oscillatory motion also introduced higher frequency components which makes the analysis challenging. The applicability of a model based on unsteady airfoil theory is also somewhat questionable, since it does not account for dynamic inflow and a rotating wake. No attempt was made to separate the true added mass from circulatory effects, which is very difficult experimentally. However, one would expect the coefficient of true added mass to be independent of frequency.

The multiple frequency oscillations were intended to replicate the form of velocity perturbation that is likely to be observed by a rotating blade in a turbulence eddy that is non-coherent over the rotor plane, or through the depth-wise shear profile of the mean flow. Rotational sampling of turbulence is likely to be a dominant contributor of tidal turbine blade fatigue. The relatively small overshoots of the bending moment that were observed at the intermediate peaks, for which the flow would most likely be attached, may be due to dynamic inflow effects. However, the loads associated with stall, which are a function of frequency and amplitude, become highly complex in cases of multi-frequency motion and again will likely necessitate the use of advanced numerical models for accurate load predictions.

VI. Conclusions

An experimental based analysis has demonstrated that the unsteady bending moment is sensitive to the oscillatory frequency and amplitude. The unsteady load component due to phenomenon associated with flow separation and dynamic stall induces load magnitudes considerably in excess of those which would be predicted using a quasi-steady based model. This will be of concern for tidal turbines which are stall regulated, or those which are likely to be exposed to unsteady flow perturbations of sufficient magnitude for the blades to enter stall. Predicting these loads will likely necessitate models capable of accounting for unsteady flow phenomena and dynamic stall.

For attached flow, the forces in phase with acceleration are likely to be of relatively small magnitude compared to those in phase with velocity. Consequently, the resulting loads can be relatively well predicted using a quasi-steady or linear model. Any unsteady effects could possibly be accounted for by the introduction of correction factor.

Acknowledgment

This research has been conducted as part of a Ph.D. program and I. A. Milne. acknowledges the financial assistance of the Bright Futures Top Achiever Doctoral Scholarship. The experimental equipment used in this study was built with the support of the UK EPSRC grant EP/F062036/1 “Feasibility of an Innovative Methodology for Testing Marine Current Turbines in Unsteady Flow”. The authors acknowledge the Department of Naval Architecture and Marine Engineering at the University of Strathclyde for technical expertise and support.

References

[1] I. A. Milne, R. N. Sharma, R. G. J. Flay, and S. Bickerton, “A preliminary analysis of the effect of the onset flow structure on tidal turbine blade loads,” in *Proceedings of Oceans’ 10, Sydney, Australia*. IEEE, May 24-27 2010.

[2] ——, “The role of onset turbulence on tidal turbine unsteady blade loads,” in *Proceedings of the 17th Australasian Fluid Mechanics Conference, Auckland, New Zealand*, December 5-9 2010.

[3] ——, “The role of waves on tidal turbine unsteady blade loading,” in *Proceedings of the 3rd International Conference on Ocean Energy, Bilbao, Spain*, October 6-8 2010.

[4] G. N. McCann, “Tidal current turbine fatigue loading sensitivity to waves and turbulence-a parametric study,” in *Proceedings of the 7th European Wave and Tidal Energy Conference, Porto, Portugal*, September 11-13 2007.

[5] A. S. Bahaj, W. M. J. Batten, and G. McCann, “Experimental verifications of numerical predictions for the hydrodynamic performance of horizontal axis marine current turbines,” *Renewable Energy*, vol. 32, no. 15, pp. 2479–2490, 2007.

[6] A. S. Bahaj, A. F. Molland, J. R. Chaplin, and W. M. J. Batten, “Power and thrust measurements of marine current turbines under various hydrodynamic flow conditions in a cavitation tunnel and a towing tank,” *Renewable Energy*, vol. 32, no. 3, pp. 407–426, 2007.

[7] W. M. J. Batten, A. S. Bahaj, A. F. Molland, and J. R. Chaplin, “Hydrodynamics of marine current turbines,” *Renewable Energy*, vol. 31, no. 2, pp. 249–256, 2006.

[8] L. Myers and A. S. Bahaj, “Power output performance characteristics of a horizontal axis marine current turbine,” *Renewable Energy*, vol. 31, no. 2, pp. 197–208, 2006.

[9] J. I. Whelan, “A fluid dynamic study of free-surface proximity and inertia effects of tidal turbines,” Ph.D. dissertation, Imperial College of Science, Technology and Medicine, Prince Consort Road London SW7 2AZ, 2010.

[10] P. W. Galloway, L. E. Myers, and A. S. Bahaj, “Studies of a scale tidal turbine in close proximity to waves,” in *Proceedings of the 3rd International Conference on Ocean Energy, Bilbao, Spain*, October 6-8 2010.

[11] N. Barltrop, K. S. Varyani, A. Grant, D. Clelland, and P. Xuan, “Wave-current interactions in marine current turbines,” *Proceedings of the Institution of Mechanical Engineers – Part M – Journal of Engineering for the Maritime Environment*, vol. 220, no. 4, pp. 195–203, 2006.

[12] D. Shipley, M. Miller, and M. Robinson, "Dynamic stall occurrence on a horizontal axis wind turbine blade," in *Proceedings of the 1995 American Society of Mechanical Engineers (ASME) energy sources technology conference and exhibition, Houston, TX (United States)*, 29 Jan - 1 Feb 1995.

[13] J. G. Leishman, "Challenges in modelling the unsteady aerodynamics of wind turbines," *Wind Energy*, vol. 5, pp. 85–132, 2002.

[14] ——, *Principles of Helicopter Aerodynamics*, 2nd ed., ser. Cambridge Aerospace. Cambridge University Press, 2006.

[15] D. Somers, "Design and experimental results for the s814 airfoil," National Renewable Energy Lab., Golden, CO (United States), NREL/SR–440-6919, January 1997.

[16] H. Sutherland, "On the fatigue analysis of wind turbines," Sandia National Laboratories, Tech. Rep., 1999.

[17] J. Morison, M. O'Brian, J. Johnson, and S. Schaaf, "The force exerted by surface waves on piles." *AIME Petroleum Transactions*, vol. 189, pp. 149–157, 1950.